SCIENCE CHINA
Life Sciences

•RESEARCH PAPER•

February 2021 Vol.64 No.2: 269–281
https://doi.org/10.1007/s11427-019-1575-x

Injectable collagen scaffold promotes swine myocardial infarction recovery by long-term local retention of transplanted human umbilical cord mesenchymal stem cells

Qiang Wang[1†], Xiaojun He[1†], Bin Wang[2†], Jun Pan[1], Chunying Shi[3], Jie Li[4], Liudi Wang[2], Yannan Zhao[5*], Jianwu Dai[5*] & Dongjin Wang[1*]

[1]*Department of Thoracic and Cardiovascular Surgery, the Affiliated Drum Tower Hospital of Nanjing University Medical School, Nanjing 210008, China;*
[2]*Center for Clinical Stem Cell Research, the Affiliated Drum Tower Hospital of Nanjing University Medical School, Nanjing 210008, China;*
[3]*Department of Human Anatomy, Histology and Embryology, School of Basic Medicine, Qingdao University, Qingdao 266021, China;*
[4]*Department of Cardiology, the Affiliated Drum Tower Hospital of Nanjing University Medical School, Nanjing 210008, China;*
[5]*Key Laboratory of Molecular Developmental Biology, Institute of Genetics and Developmental Biology, Chinese Academy of Sciences, Beijing 100190, China*

Received September 23, 2019; accepted October 25, 2019; published online July 23, 2020

Stem cell therapy is an attractive approach for recovery from myocardial infarction (MI) but faces the challenges of rapid diffusion and poor survival after transplantation. Here we developed an injectable collagen scaffold to promote the long-term retention of transplanted cells in chronic MI. Forty-five minipigs underwent left anterior descending artery (LAD) ligation and were equally divided into three groups 2 months later (collagen scaffold loading with human umbilical mesenchymal stem cell (hUMSC) group, hUMSC group, and placebo group (only phosphate-buffered saline (PBS) injection)). Immunofluorescence staining indicated that the retention of transplanted cells was promoted by the collagen scaffold. Echocardiography and cardiac magnetic resonance imaging (CMR) showed much higher left ventricular ejection fraction (LVEF) and lower infarct size percentage in the collagen/hUMSC group than in the hUMSC and placebo groups at 12 months after treatment. There were also higher densities of vWf-, α-sma-, and cTnT-positive cells in the infarct border zone in the collagen/cell group, as revealed by immunohistochemical analysis, suggesting better angiogenesis and more cardiomyocyte survival after MI. Thus, the injectable collagen scaffold was safe and effective on a large animal myocardial model, which is beneficial for constructing a favorable microenvironment for applying stem cells in clinical MI.

injectable collagen scaffold, mesenchymal stem cell, MI

Citation: Wang, Q., He, X., Wang, B., Pan, J., Shi, C., Li, J., Wang, L., Zhao, Y., Dai, J., and Wang, D. (2021). Injectable collagen scaffold promotes swine myocardial infarction recovery by long-term local retention of transplanted human umbilical cord mesenchymal stem cells. Sci China Life Sci 64, 269–281. https://doi.org/10.1007/s11427-019-1575-x

INTRODUCTION

Myocardial infarction (MI), usually as a result of coronary atherosclerosis (Thygesen et al., 2012), causes myocardial cell loss and hyperplastic nonfunctioning scar tissue, resulting in heart failure (Sepantafar et al., 2016). MI is a major cause of mortality and morbidity worldwide (Paiva et al., 2015). Effective treatment strategies for MI include limiting adverse ventricular remodeling, attenuating myocardial scar expansion, and enhancing cardiac functions and myocardial regeneration (Chen et al., 2020; Perea-Gil et al., 2015; Dixit

†Contributed equally to this work
*Corresponding authors (Yannan Zhao, email: ynzhao@genetics.ac.cn; Jianwu Dai, email: jwdai@genetics.ac.cn; Dongjin Wang, email: wangdongjin@njglyy.com)

and Katare, 2015).

It is widely believed that the adult heart is a terminally differentiated organ with very limited self-renewal capacity after injury (Beltrami et al., 2001). Although recent analyses have shown that adult cardiomyocytes can reenter the cell cycle and form new myocytes after MI, the innate regenerative capacity of cardiomyocytes is very low and declines significantly with aging, further reducing the likelihood of the recovery of damaged tissue (Mahmoudi et al., 2017). Stem cell-based therapies represent an exciting option for repairing injured heart and have attracted considerable attention over the last 15 years. Multiple cell types, including human embryonic stem cells, skeletal myoblasts, bone marrow stem cells, induced pluripotent stem cells, and mesenchymal stem cells (MSCs), have been employed to remuscularize the injured heart (Dixit and Katare, 2015; Nguyen et al., 2016). Accumulating evidence indicates that infusion, injection, or tissue-based implantation of stem cells derived from various origins is safe and confers therapeutic benefits to the injured heart (Eschenhagen et al., 2017), via cellular cross-talk (Bollini et al., 2018) and paracrine mechanisms (Sanganalmath and Bolli, 2013). However, the effectiveness of cell transplantation is hampered by poor retention, survival, and proliferation of the transplanted cells in heart tissue (Sepantafar et al., 2016; Mahmoudi et al., 2017), with only approximately 1%–20% of transplanted cells surviving after transplantation, significantly limiting their therapeutic potential (Marquardt and Heilshorn, 2016).

Co-injection of scaffolding materials and the use of tissue engineering approaches may help to reduce these effects (Wall et al., 2010). Cell-based tissue engineering approaches have thus attracted considerable attention as a therapeutic option for heart failure (Buikema et al., 2013; Radhakrishnan et al., 2014; Sepantafar et al., 2016). Cell-based biomaterial gels are applied as either an injectable cell-laden gel or a cardiac patch sewn onto the infarct area of the heart (Sepantafar et al., 2016). Sufficient small animal studies, translational large animal studies (Araña et al., 2014; Shafy et al., 2013), and clinical trials (Chachques et al., 2007; Chachques et al., 2008) have been performed for the collagen-based cardiac patch approach. However, most of the studies (Perea-Gil et al., 2015) about injectable cell-laden hydrogels, especially collagen-derived ones, were performed in small animals (mice or rats). There has thus been a lack of investigations in large animal models, which can more closely mimic the cardiac pathophysiology of human patients. Therefore, we here adopted a large animal (swine) infarction model to assess the effect of cell-laden injectable collagen hydrogel on cardiac regeneration.

Collagen, as the predominant protein in the mammalian extracellular matrix (ECM), provides structural support for maintaining tissue integrity and contributes to the specificity of the ECM microenvironment (Gelse et al., 2003) for cell adherence and amplification (Shi et al., 2011; Wang et al., 2007). Several properties of collagen, including its biocompatibility, adhesiveness, and biodegradability, have made it an appropriate natural scaffold material for applications in regenerative medicine (Jiang et al., 2019; Chiu et al., 2012; Gautam et al., 2014; Kijeńska et al., 2012; Perea-Gil et al., 2015; Xu et al., 2014). Collagen scaffolds have been used in cardiac tissue engineering and been shown to promote cardiac commitment, vascularization, and electrical coupling in different MI models (Perea-Gil et al., 2015). Observations of negative ventricular remodeling prevention, heart function reversion, and angiogenesis increase have been described in the literature (Araña et al., 2014; Araña et al., 2013; Blackburn et al., 2015; Chachques et al., 2007; Chachques et al., 2008; Gaballa et al., 2006; Holladay et al., 2012; Maureira et al., 2012; Mokashi et al., 2010; Serpooshan et al., 2013; Shafy et al., 2013; Xiang et al., 2006).

We previously revealed that implantation of a collagen-binding human vascular endothelial growth factor-collagen membrane patch into the infarcted myocardium could effectively improve left ventricle (LV) cardiac function and increase vascular density (Gao et al., 2011). We also developed sca-1 antibody-conjugated collagen to capture native autologous stem/progenitor cells for cardiac tissue regeneration (Shi et al., 2011). Here, we study the effect of a collagen scaffold as a stem cell transplantation vehicle in a permanent MI large animal (swine) model. Our results revealed that the collagen scaffold was safe and feasible for intramyocardial treatment with stem cells. The collagen scaffold can enhance stem cell retention at the site of delivery, prevent MI scar enlargement, help in the recovery of cardiac function, and promote angiogenesis and tissue survival. This work thus provides evidence for the clinical application of collagen hydrogel-based stem cell therapy for cardiac regeneration.

RESULTS

The whole study protocol was descripted as below (Figure 1).

Characterization of injectable collagen scaffold and clinical-grade hUMSCs

The injectable porous collagen scaffold was a white viscous gel, and scanning electron microscopy (SEM) analysis indicated that it was composed of collagen fibers (Figure 2A and B). The rheological characteristics of the collagen scaffold were analyzed. An oscillatory frequency sweep of the collagen scaffold performed from 0.1 to 1 Hz showed typical hydrogel storage moduli (G′) that were higher than the loss moduli (G″) in the entire frequency range. The decrease in complex viscosity with the increase in frequency

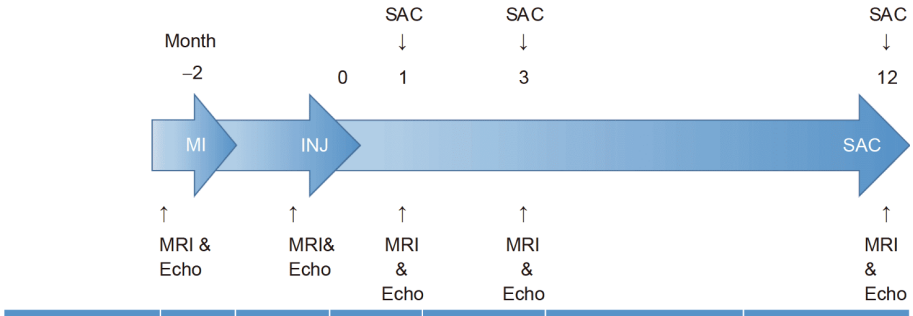

Placebo	15	15	15	10		5
Cell	15	15	15	10		5
Collagen/cell	15	15	15	10		5

Figure 1 Timeline of animal study. MRI, magnetic resonance imaging; SAC, sacrifice; MI, coronary artery ligation; INJ, injection of hUMSCs with or without collagen scaffold.

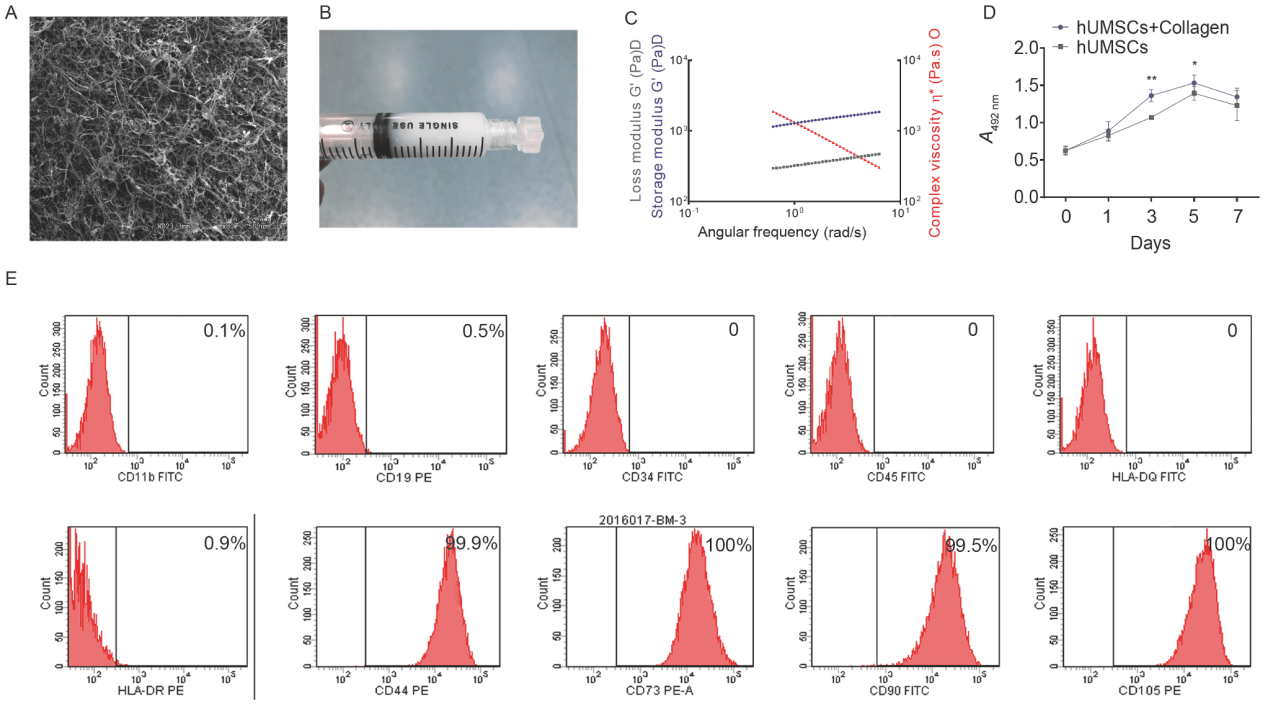

Figure 2 Characterization of injectable collagen scaffold and clinical-grade hUMSCs. A, SEM of injectable collagen gel displayed fibrillar networks of collagen fibers suitable for cell attachment. Scale bar: 500 μm. B, Injectable collagen gel mixed with hUMSCs for injection. C, Storage (G′) moduli (blue), loss (G″) moduli (green), and complex viscosity (red) of the collagen scaffold. D, Viability of hUMSCs cultured routinely (placebo group) or co-cultured in collagen (collagen group) *in vitro*. E, High expression of typical MSC markers CD73, CD90, and CD105, but lack of expression of CD34, CD45, CD14, CD19, and HLA-DR, assayed by flow cytometry. Graphs represent mean±standard deviation. *, $P \leq 0.05$, **, $P \leq 0.001$, *t*-test.

indicated the shear-thinning phenomenon (Figure 2C). The biological safety of the collagen scaffold was evaluated by authorized third-party inspection by the China Food and Drug Administration, and it was shown to meet the Chinese Criterion for Medical Devices GB16886 regarding the absence of allergens and biological toxicity.

Clinical-grade hUMSCs were isolated from human umbilical cords and shown to be positive for MSC markers (CD44, CD73, CD90, and CD105) and negative for markers (CD11b, CD19, CD34, CD45, HLA-DR, and HLA-DQ) by flow cytometry analysis (Figure 2E). Fourth- to fifth-passage hUMSCs were used in our study.

We investigated the effects of the injected collagen scaffold on hUMSCs *in vitro* by assessing the metabolic activities of cells cultured in cell culture dishes with or without collagen scaffold pre-coating. Co-culture with the collagen scaffold did not decrease the cellular viability of hUMSCs compared with the normal hUMSC culture, according to the MTT assay results, with significant differences on days 3 and 5 compared with the control group. This indicated that the

collagen scaffold was not cytotoxic (Figure 2D).

Safety assessment

There were no adverse events such as death or infection observed after collagen scaffold and hUMSC implantation. Blood analyses of alanine transaminase (ALT), aspartate aminotransferase (AST), blood urea nitrogen (BUN), creatinine (Cr), hemoglobin (Hb), lactate dehydrogenase (LDH), platelets (Plt), red blood cells (RBCs), and white blood cells (WBCs) were performed at 1 week, 1 month, and 12 months after transplantation (Figure 3). No significant differences were observed among control, hUMSC, and collagen/hUMSC groups.

Restoration of cardiac function and attenuation of LV remodeling

Global changes in LV function, chamber dimensions, and scar size were assessed by cardiac magnetic resonance imaging (CMR) and echocardiography (Figure 4). Both echocardiography and CMR revealed better LV function with higher ejection fraction (EF) (Figure 4A and B). Left ventricular ejection fraction (LVEF) decreased after MI and then increased after treatment in the animals in the treated group, but remained depressed in the placebo group (baseline versus 3 months: 44.48%±5.86% versus 52.55%±5.47% in the collagen/cell group, P=0.027; 42.44%±4.05% versus 50.53%±7.26% in the cell group, P=0.001; and 44.58% ±2.68% versus 43.88%±2.89% in the placebo group, P=0.495; based on CMR). The CMR EF was higher in the collagen/hUMSC group than in the hUMSC group and placebo group after treatment (52.55%±5.47%, 50.53%±7.26%, 43.88%±2.89%, respectively; P<0.01) (Figure 4B).

In addition, cardiac output was significantly higher in the collagen/hUMSC group than in the hUMSC and placebo groups at 12 months after injection ((2.32±0.28) L, (1.60 ±0.08) L, (1.59±0.13) L, respectively; P<0.001) (Figure 4C). Stroke volume followed the same trend as cardiac output (Figure 4D).

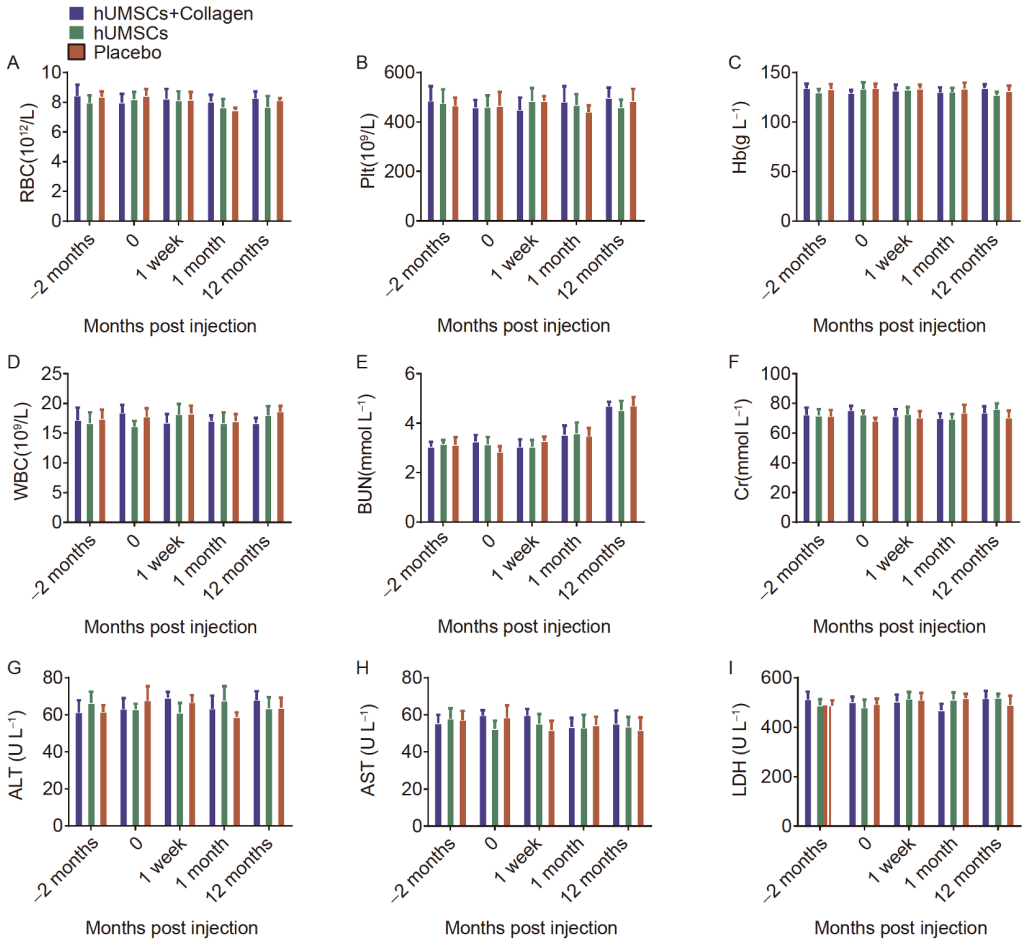

Figure 3 Safety of injectable collagen scaffold and hUMSC implantation in swine with MI. There were no significant differences in blood test parameters among pigs in the different groups pre-infarction (−2 months), pre-injection (0), and at 1 week, 1 month, and 12 months after injection, indicating the safety of the injectable collagen scaffold and hUMSCs. A, RBC, red blood cell. B, Plt, platelet. C, Hb, hemoglobin. D, WBC, white blood cell. E, BUN, blood urea nitrogen. F, Cr, creatinine. G, ALT, alanine transaminase. H, AST, aspartate aminotransferase. I, LDH, lactate dehydrogenase.

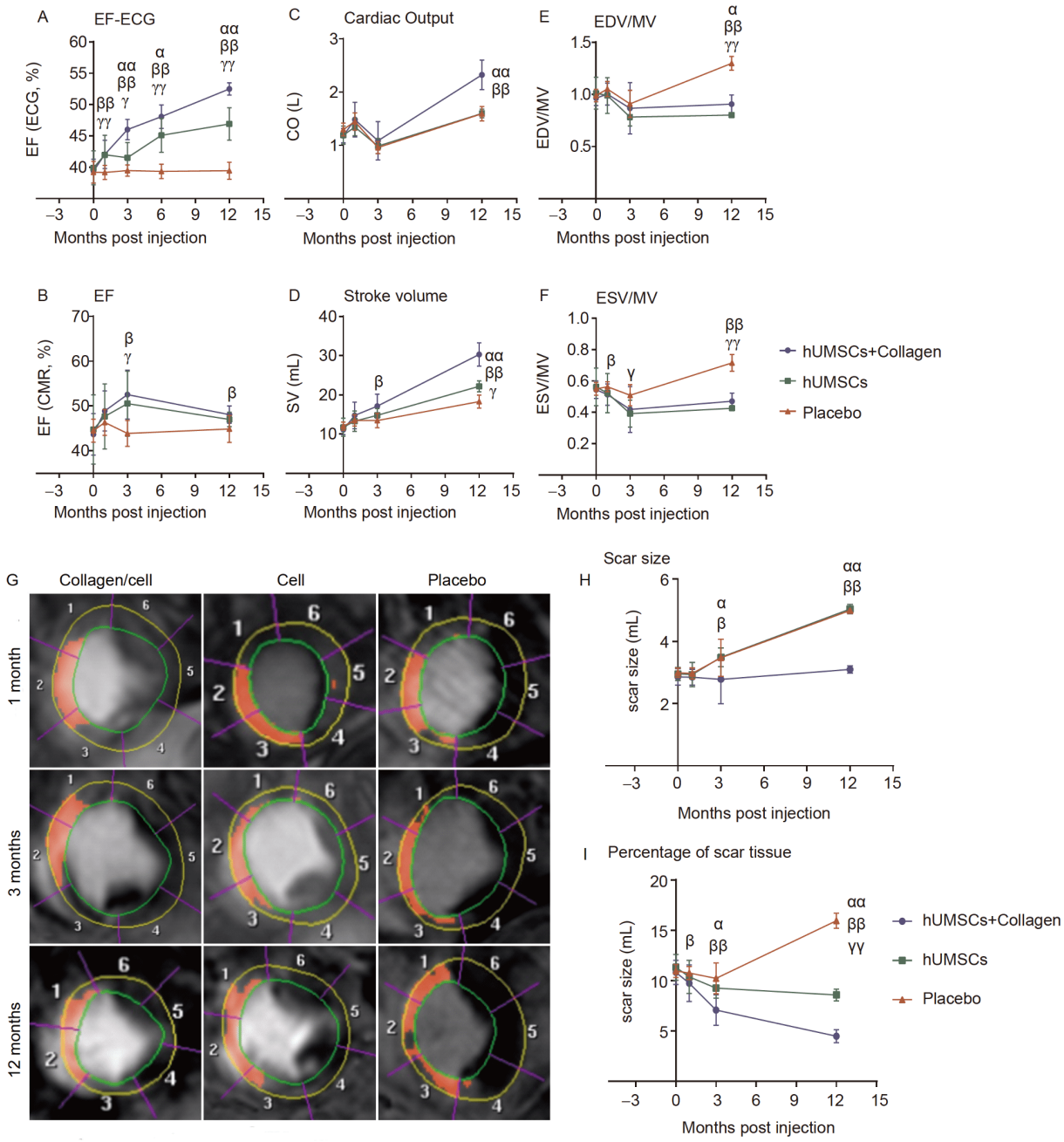

Figure 4 Restoration of cardiac function, attenuation of negative LV remodeling, and prevention of scar tissue enlargement after hUMSC/collagen treatment. MRI results for cardiac function, cardiac size, and scar tissue. In the hUMSC/collagen group, cardiac function was improved (A–D), negative LV remodeling was attenuated (E, F), and scar tissue enlargement was prevented (G–I) compared with the status in the hUMSC and placebo groups. G, Representative delayed-enhancement CMR end-systolic short-axis images. Graphs present mean±standard deviation. Collagen/hUMSC versus hUMSC group: α, $P \leq 0.05$, αα, $P \leq 0.001$. Collagen/hUMSC versus placebo group: β, $P \leq 0.05$, ββ, $P \leq 0.001$. hUMSC versus placebo group: γ, $P \leq 0.05$, γγ, $P \leq 0.001$. EF, ejection fraction; EDV, end-diastole volume; ESV, end-systolic volume; MV, myocardial volume.

Evaluation of LV dimensions in relation to maladaptive LV remodeling revealed better outcomes overall after collagen/cell therapy (Figure 4E and F). End-diastolic volume (EDV) and end-systolic volume (ESV) after adjusting for the increase in total left ventricular myocardial volume (MV) in the treated groups were significantly lower than in the placebo group. This was due to animal growth during follow-up, suggesting a reduction in LV remodeling and increased contractility.

Change of cardiac scar tissue

Delayed-enhancement CMR was used to measure changes in absolute scar mass and infarct size as a percentage of LV mass volume (LVMV) (Figure 4G–I). There were no significant differences in heart rate among the three groups

under the same conditions of anesthesia. From preinjection to 12 months after cell injection, the increase in infarct size (absolute scar mass) in the collagen/hUMSC group (1.11% ±2.72%) was significantly less than that in the hUMSC and placebo groups (57.03%±4.39% and 63.56%±7.05%, respectively; both $P<0.001$) (Figure 4G and H). Furthermore, the infarct size measured as a percentage of LVMV decreased in the collagen/hUMSC ($P<0.001$) and hUMSC groups ($P<0.001$) from preinjection to 12 months after treatment, but increased in the placebo group ($P<0.001$) (Figure 4I). The preinjection infarct sizes as a percentage of LV mass were 10.82%±1.20%, 11.32%±1.29%, and 10.96% ±0.65% in the collagen/hUMSC, hUMSC, and placebo groups, respectively ($P=0.383$), compared with 4.47% ±0.65%, 8.58%±0.59%, and 15.95%±0.76% ($P<0.001$) at 12 months (Figure 4I). The large decrease in infarct size percentage may have been the major contributor to the restoration of cardiac function after cell therapy.

Intramyocardial retention of hUMSCs in swine with MI

To explore whether the collagen scaffold could promote transplanted cell retention and survival in heart tissue, transplanted hUMSCs in swine hearts were traced by immunofluorescence staining with anti-human nuclear antigen antibody (HUNU). Cells with positive staining for HUNU were ten-fold the level in the cell transplantation group at 1 months and nearly double at 3 months after treatment, suggesting that the collagen scaffold significantly promoted retention of the transplanted cells in the heart (green markers in Figure 5). There were numerous HUNU-positive cells in the collagen/hUMSC group hearts at 1 month after treatment, which decreased sharply as time passed, suggesting their loss from heart tissue.

Red markers in Figure 6 indicate α-sma-positive cells. From the circular shapes and visible lumen, we recognize most of these cells as part of the arterioles, indicating the correlation between transplanted hUMSCs and artery renewal in the cardiac infarct zone.

Neo-angiogenesis and myocardial tissue survival

To detect neo-angiogenesis, we used α-SMA and vWf antibody staining to identify arterioles and capillaries. Immunohistochemical analysis revealed that the density of arterioles was higher in the collagen/hUMSC group than in the hUMSC and placebo groups at 1, 3, and 12 months. There was no significant difference between the collagen/hUMSC and hUMSC groups, but the density was significantly ($P<0.001$) lower in the placebo group (Figure 6A). The density of vWf-positive cells peaked at the third month postinjection in the collagen/hUMSC group, which was significantly higher than that in the hUMSC alone and placebo groups ($P<0.05$, Figure 6B).

The density of island- or strip-shaped cTnT-positive myocardial cells in the scar tissue was higher in the collagen/hUMSC group than in the hUMSC and placebo groups (Figure 7). These results indicated that neo-angiogenesis and

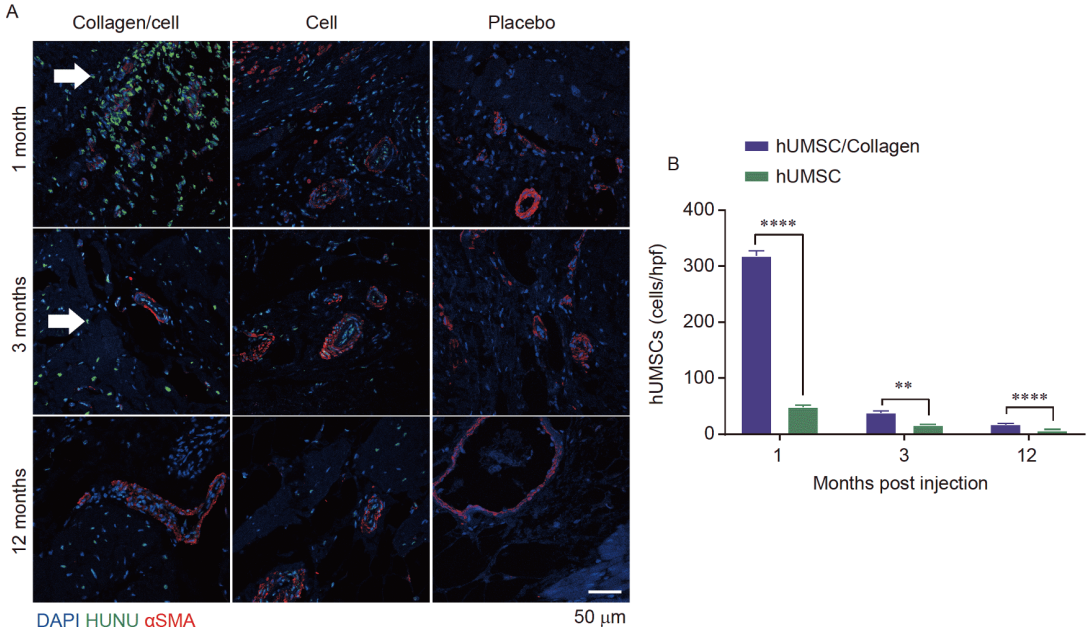

Figure 5 Intramyocardial retention of hUMSCs in pigs with MI. A, Immunofluorescence co-staining with anti-human nuclear antigen antibody (HUNU, green) and anti-α-SMA (red) showed more HUNU-positive cells in the collagen/hUMSC group than in the hUMSC group. Some of the transplanted cells were involved in angiogenesis (white arrows). B, Quantified HUNU-positive cells in the collagen/hUMSC and hUMSC groups. Graphs present mean ±standard deviation. *, $P\leq0.05$, **, $P\leq0.01$, ***, $P\leq0.001$, *t*-test. hpf, high-power field.

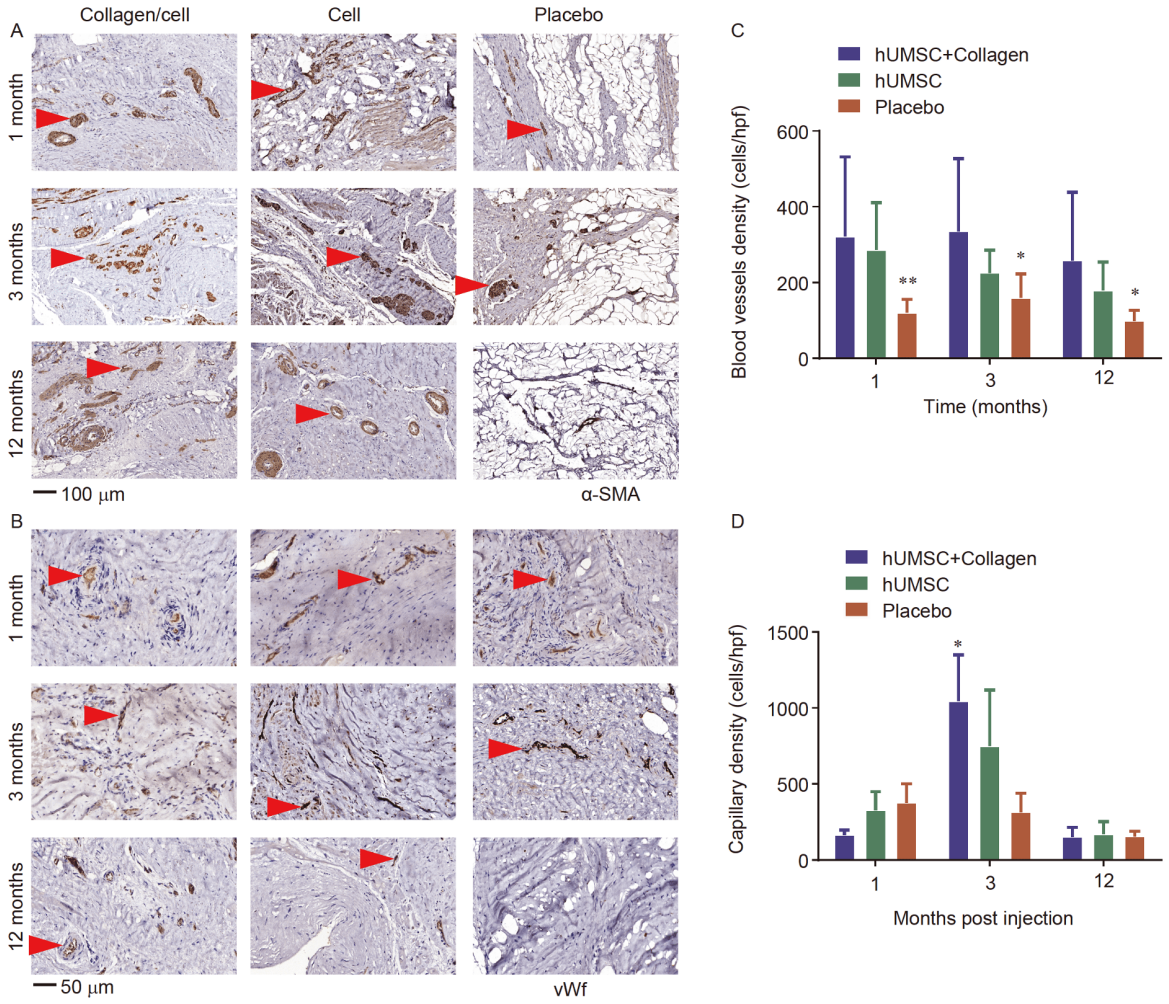

Figure 6 Neo-angiogenesis after hUMSC/collagen treatment. A and C, Anti-α-SMA antibody staining for identifying large vessels. Staining showed higher densities of α-SMA-positive cells in the collagen/hUMSC and hUMSC groups than in the placebo group at the indicated times. B and D, Anti-vWf antibody staining for identifying capillaries. Immunohistochemical analysis revealed that the density of vWf-positive cells in the collagen/hUMSC group peaked at 3 months after injection, but did so later in the hUMSC and placebo groups. Graphs present mean±standard. *, $P \leq 0.05$, **, $P \leq 0.01$, ***, $P \leq 0.001$, *t*-test.

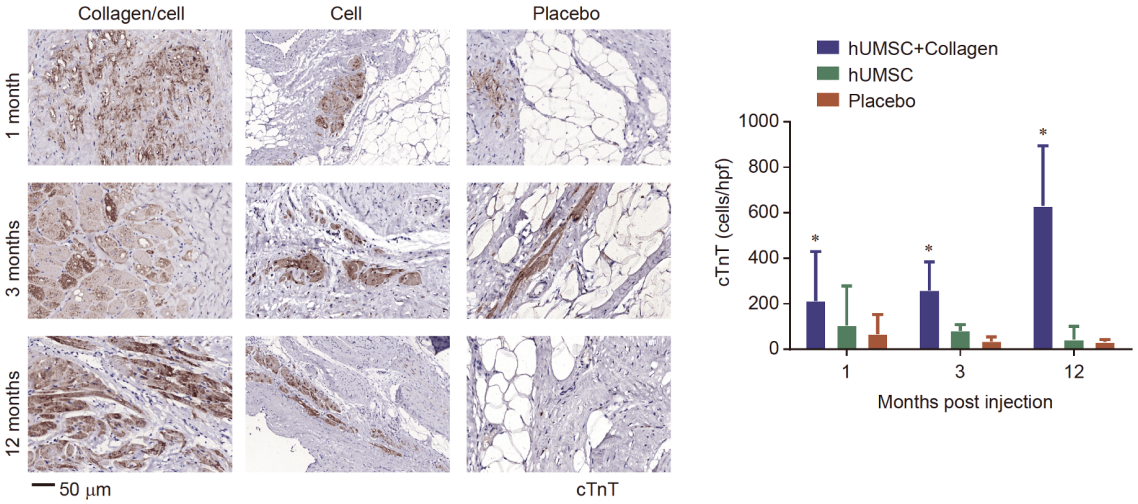

Figure 7 Collagen/hUMSC transplantation enhanced myocardial tissue survival. The number and density of island- or strip-shaped cTnT-positive myocardial cells in the scar tissue were higher in the collagen/hUMSC group than in the hUMSC and placebo groups, as determined by anti-cTnT antibody staining. Graphs present mean±standard. *, $P \leq 0.05$, **, $P \leq 0.01$, ***, $P \leq 0.001$, *t*-test.

cell survival occurred in the hUMSC groups and were promoted by collagen.

DISCUSSION

The limited regenerative capability of cardiac tissue presents a major difficulty for the conventional clinical treatment of cardiac injuries. Cell therapy is an exciting option aimed at overcoming this problem, and many studies have suggested that the implantation of cells of various origins can confer therapeutic benefits to the injured heart.

Numerous studies have investigated the use of stem cell therapies for MI and chronic heart failure, but currently available data have indicated heterogeneous outcomes and limited improvements in cardiac performance. Jansen Of Lorkeers et al. (2015) performed a meta-analysis of stem cell therapy for MI in large animals and showed an absolute difference in LVEF of 8.3% between treated and control animals, with an LVEF of −7.83% to 22.6%.

The major problem is that retention and survival of cells post-injection remain low, which continues to limit cell therapy for cardiac repair (Eschenhagen et al., 2017; Mahmoudi et al., 2017). Current approaches are characterized by the loss of most of the transplanted stem cells through apoptosis or their poor retention post-delivery, potentially offsetting their long-term efficacy (Golpanian et al., 2016; Keith et al., 2015). These effects may be partially caused by the lack of appropriate space in the dense myocardial tissue, which is an inhospitable environment for the therapeutic cells (Behfar et al., 2014). These problems might be solved by injectable hydrogels as a cell delivery vehicle to promote cell retention and survival (Sepantafar et al., 2016). Numerous studies on this issue have been performed, most of which were based on small animals (Perea-Gil et al., 2015; Wu et al., 2019).

Only a few large animal studies on injectable hydrogel combined with cell therapy for MI have been performed. For example, Lin et al. (2010) reported that intramyocardial peptide nanofiber injection could improve the efficacy of bone marrow cell therapy in post-infarction pigs. Improvements of systolic and diastolic function occurred, along with a nearly 7.8-fold increase of cell retention and promoted capillary density in the nanofiber complex cell group at 4 weeks after treatment. The treatment was applied immediately after MI induction. This is very different from our study, in which collagen and/or cells were delivered 2 months after MI. In the study of Chen et al. (2014), hyaluronan hydrogel and bone marrow cells were injected 10 min after coronary artery ligation. In addition, Chang et al. (2016) studied the effect of intramyocardial injection with hyaluronan hydrogel and human cord blood cells 24 h after MI induction. Both of these studies reported higher LVEF, lower infarct size, and nearly twofold greater cell retention in the hyaluronan hydrogel complex cell group than in the cell group at 2 months after treatment.

Collagen, as a natural biomaterial, has been used in regenerative therapy such as spinal cord injury repair (Han et al., 2018; Lin, 2019; Shen et al., 2019).

To the best of our knowledge, this study is the first large animal study about collagen-based cell-laden injectable hydrogel for MI. In this study, immunofluorescence co-staining with anti-human nuclear antigen antibody indicated that injection of the collagen scaffold could markedly increase the retention of hUMSCs at the transplant site. This effect of promoting cell retention resembles that in previous studies based on hyaluronan hydrogel and peptide nanofibers. Future research is needed to determine the most suitable material.

In the current study, we evaluated the effects of collagen scaffold and hUMSC treatment on cardiac function and LV remodeling in pigs using CMR. LVEF decreased after MI and recovered after treatment in the treated pigs. Jeevanantham et al. (2012) compared different imaging modalities for assessing cardiac function following cardiac regenerative therapy, in a total of 50 clinical trials (2,625 patients). Improvements of LVEF in bone marrow stem cell (BMC)-treated patients were more significant when assessed by echocardiography or left ventriculography (LVG) compared with SPECT or MR; infarct scar size reduction was significant with both SPECT and LVG, but not with magnetic resonance imaging (MRI). Meanwhile, reduction in LVESV was significant with all imaging modalities, although the magnitude varied, whereas reduction in LVEDV was significant by echocardiography and SPECT, but not by MRI or LVG. The current study shows a reduction in ESV/LVMV and increase in LVEF by CMR, which are consistent with the literature, and suggests that collagen scaffolds could be useful to attenuate cardiac remodeling.

Although there was no reduction of scar size measured by delayed gadolinium enhancement in any of the groups in the current study, the scar size was unchanged in the collagen/hUMSC group, but was significantly increased in the other two groups, suggesting that the injectable collagen hydrogel loaded with hUMSCs could prevent the amplification of scar tissue. This result differed from those in other cardiac regenerative studies, most of which demonstrated reduced scar size. However, we carried out implantation of the scaffold and hUMSCs at 2 months after MI, and it is possible that this inhibited scar amplification but could not reverse the scar volume at this stage. Therefore, cardiac function restoration may not arise from tissue regeneration in the scar area, even though the density of island- or strip-shaped cTnT-positive myocardial cells in the scar tissue was higher in the collagen/hUMSC group than in the others.

Pigs in the collagen/hUMSC group showed greater neo-

angiogenesis and cardiomyocyte survival than pigs in the hUMSC and placebo groups, coupled with changes in cardiac function and scar size. Notably, the peak of neo-angiogenesis (indicated by vWf) occurred at 3 months after transplantation in the collagen/hUMSC group, while cTnT-positive cells peaked at 12 months, suggesting vessel renewal, and might have resulted from micro-environmental improvements following biomaterial transplantation.

Cell retention after transplantation into the myocardium may also be affected by the route of cell delivery (Eschenhagen et al., 2017). There are four major clinically practical routes (Fukushima et al., 2013): intramyocardial injection, intracoronary injection, intravenous injection, and epicardial placement of "cell sheets." Epicardial placement of cell sheets resulted in poor cell integration into the myocardium, intravenous injection was associated with low cell recruitment into the heart, and intracoronary injection was also limited by poor initial cell retention in the heart (Fukushima et al., 2013). Hou et al. (2005) evaluated the short-term fate of peripheral blood mononuclear cells after intramyocardial, intracoronary, and interstitial retrograde coronary venous delivery in an ischemic swine model, and showed that intramyocardial injection was more efficient, even though most of the delivered cells were not retained in the heart following any of the tested delivery modalities.

Besides, the optimal timing for stem cell therapy following MI remains unclear, and meta-analyses have reported inconsistent results. Preclinical studies (Jansen of Lorkeers et al., 2015) showed no significant differences in relation to the time of administration (<1 day, 1–7 days, >7 days after acute MI), while clinical trials (Jeevanantham et al., 2012) revealed similar improvements in LVEF, infarct scar size, and LVESV between <7 days and 7–30 days after acute MI. Another meta-analysis of acute MI trials reported a greater improvement in LVEF with BMC injection >7 days after acute MI (Martin-Rendon et al., 2008), while a recent meta-analysis (Liu et al., 2016) found that the optimal timing for cell therapy was 4–7 days after acute MI. A very recent study (Xu et al., 2019) reported that mid-term stage (7–14 days) after acute MI could be optimal. However, even though more and more patients with acute MI can receive reperfusion therapy, there are still many patients experiencing MI for >30 days without early reperfusion, thus exhibiting adverse ventricular remodeling and scar formation. To explore treatment for these patients with old cardiac infarction, we used the intramyocardial route at 2 months after establishment of a permanent LAD occlusion MI model instead of an ischemia reperfusion model to explore the effect of collagen scaffold hydrogel on cell-based cardiac regenerative therapy.

Overall, the results of the present study indicated that intramyocardial injection of a collagen scaffold loaded with hUMSCs was a safe procedure in a pig model of MI. This technique enhanced improvements in global LV systolic function and LVEF coupled with a decrease in scar tissue percentage, associated with increased retention of the transplanted cells and neo-angiogenesis at the scar area. These results therefore suggest that the combination of hUMSCs and collagen scaffolds might be a safe and effective therapeutic option for myocardial infarction with LV dysfunction, via the construction of a microenvironment that promotes regeneration.

MATERIALS AND METHODS

Chinese Pama minipigs (females, 15–20 kg, age 6 months) underwent experimental MI (as described below), followed by the injection of collagen scaffold and hUMSCs, hUMSCs without collagen scaffold, or PBS (Figure 1). For all procedures, pigs were anesthetized by intramuscular injection with a mixture of xylazine hydrochloride (2 g), atropine sulfate (0.5 mg), and droperidol (5 mg), followed by intravenous propofol (200 mg in 100 mL of a 5% glucose solution). The animals were intubated using a tracheal tube (5 mm diameter) and ventilated with a Siemens 900C respirator (Siemens AG, Munich, Germany) (volume 14 mL kg^{-1}, frequency 24 breaths per min, inspired oxygen fraction 100%). Blood pressure, electrocardiogram (ECG), and oxygen saturation were monitored during surgery.

Cell isolation and expansion

hUMSCs were isolated from neonatal human umbilical cord Wharton's jelly and expanded, as described previously (Zhao et al., 2017). Briefly, the cords were dissected and the blood vessels were removed. Then, the remaining tissues were cut into small pieces and digested with collagenase (Sigma-Aldrich, USA) for 18 h, followed by digestion with 0.25% trypsin (Sigma-Aldrich). The undigested tissue was removed from the cell suspension using a 100 μm filter. Cells were seeded in Dulbecco's modified Eagle's medium (Gibco, USA) comprising KnockOut™ serum supplement (Gibco), 2 mmol L^{-1} glutamine (Gibco), and 50 U penicillin/streptomycin (Gibco). Cells were cultured in a humidified atmosphere with 5% CO_2 at 37°C. After 3 days of culture, the medium was replaced to remove non-adherent cells, and the cells were passaged when they reached confluence. Microbiological and cytogenetic safety was ensured throughout the preparation process.

The cells were cultured in a Good Manufacturing Practice facility and underwent stringent quality assessment, including assays for surface markers and differentiation potential. Surface markers of hUMSCs were assessed using a FC500 flow cytometer (BD Biosciences, USA) using anti-CD11b, -CD19, -CD34, -CD45, -HLA-DQ, -HLA-DR, -CD44, -CD73, -CD90, and -CD105 antibodies.

Preparation of injectable collagen scaffold

Injectable collagen scaffolds were prepared from bovine collagen tissues. Fresh bovine aponeurosis was harvested and treated with 1% tri(n-butyl) phosphate for 48 h. Then, collagen materials were immersed in 1% trypsin for 1 h to remove cells and other proteins. After washing with deionized water, collagen was dissolved in 0.5 mol L^{-1} acetic acid for 24 h and dialyzed in deionized water for 10 days, then lyophilized and dissolved in saline to form a 30 mg mL^{-1} injectable collagen scaffold. Allergen detection and assays for acute toxicity, cytotoxicity, sub-chronic toxicity, intradermal irritation, genetic toxicity, hemolytic toxicity, and degradation were performed by the National Institute of Food and Drug Control according to the Chinese Criterion for Medical Devices GB16886, to evaluate the biological safety of the injectable collagen scaffold. Injectable collagen scaffolds were lyophilized, sputter-coated with gold, and observed by SEM (S-3000N SEM; Hitachi, Japan).

Rheological characteristics of the collagen scaffold were quantified by monitoring the storage moduli (G′) and loss moduli (G″) using a DHR-2 rheometer (TA instrument) at 25°C in the dynamic oscillatory mode with a frequency sweep from 0.1 to 1 Hz at 1% strain.

Co-culture of hUMSCs and collagen scaffold

To explore the effect of collagen on the cellular metabolic activity of hUMSCs, the cells were cultured alone (control group) or co-cultured with the collagen scaffold preparation (collagen group) *in vitro*. Collagen scaffold (200 μL) was added to each well of a 48-microwell plate. hUMSCs were re-suspended in complete medium containing 10% fetal bovine serum and fibroblast growth factor and seeded at a density of 3,000 cells per well in the 48-microwell plate; 500 μL of complete medium was added to each well. hUMSCs were then cultured in a humidified atmosphere with 5% CO_2 at 37°C. The optical density value (492 nm) was measured using the MTT method every day until day 7. For the MTT test, 60 μL of MTT (5 mg mL^{-1} in PBS) was added and the supernatant was discarded 4 h later, followed by the addition of 200 μL of dimethyl sulfoxide in the dark for 20 min.

MI and hUMSC transplantation

We used an open-chest, permanent protocol to generate a model of anterior wall MI (Shiba et al., 2016). The pericardium was opened via a left mini-thoracotomy through the fifth intercostal space. The left anterior descending (LAD) coronary artery was ligated with a 5.0 prolene suture, distal to the origin of the second diagonal branch, to produce a transmural MI. MI was confirmed by ST-segment elevation. Before the induction of MI, the pigs were administered 1 mg kg^{-1} lidocaine and 1,000 U heparin intravenously. To reduce the risk of ventricular fibrillation, 1 mg min^{-1} amiodarone was administered intravenously from ligation to the end of the surgical procedure. A 12F chest tube was inserted into the left pleural cavity via the port incision and tunneled through the chest wall. All incisions were closed in layers, and the chest tube was placed at −20 cm of underwater suction to evacuate the pneumothorax. Fluoroscopy was performed to confirm lung expansion, and the chest tube was removed before extubation. Animals were allowed to recover and provided with adequate postoperative analgesia with a transdermal fentanyl patch (75 μg h^{-1}) for 3 days.

Two months after MI, animals underwent directly visualized intramyocardial injection of collagen and/or hUMSCs. A right mini-thoracotomy was created with a small 4–5 cm incision in the fifth anterior intercostal space. The pericardium was opened, and the infarct area was identified by tissue coloration, wall motion abnormalities, and correlation with coronary anatomy. Pigs in the placebo group received 2 mL of PBS injected into the center and border zone of the infarct scar, with 10 separate injections in the border zone of the infarct scar. Pigs in the collagen/hUMSC group (15 pigs) were injected with 1.5 mL of hUMSCs (1×10^8) in PBS mixed with 0.5 mL of collagen scaffold. Another 15 pigs (hUMSC group) were administered hUMSCs (1×10^8) in 2 mL of PBS. Postoperative management was the same as after the MI procedure. Animals were euthanized at 1, 3, and 12 months after injection by the internal jugular vein injection of potassium chloride (20 mL) while in an unconscious state, after 15 min of anesthesia induced by intramuscular injection of a mixture of xylazine hydrochloride (2 g), atropine sulfate (0.5 mg), and droperidol (5 mg).

Echocardiography

Before the echocardiographic study, pigs were anesthetized (isoflurane) and placed in the left lateral decubitus position. Echocardiography was performed with a 2.5–5 MHz linear transducer and a cardiovascular ultrasound system (Philips Medical Systems CX50 model xMatrix; Royal Philips, Netherlands). The parasternal long-axis, parasternal short-axis, and apical four-chamber views were used to obtain 2D, M-mode, and spectral Doppler images. Systolic and diastolic anatomic parameters were obtained from M-mode tracings at the mid-papillary level. Digital images were analyzed off-line by a single blinded observer using ProSolv (version 2.5) image analysis software (Problem Solving Concepts, Inc., USA). EDV, ESV, stroke volume, and EF were measured.

Cardiovascular magnetic resonance studies

CMR was performed by investigators who were blinded to

the allocation of injections. These analyses were conducted using a 1.5-T scanner (Royal Philips, Netherlands) with Syngo magnetic resonance software, with an eight-channel phased-array surface coil with ECG gating and ventilator breath-holding acquisitions. Cine-MRI acquisitions were performed using a balanced fast field echo sequence in the long-axis (two-chamber and four-chamber views) and short-axis orientations with the following parameters: 3.5 ms repetition time (TR), 1.7 ms echo time (TE), 45° flip angle (FA), 320 mm×320 mm field of view (FOV), and 8 mm slice thickness. LVEF, left ventricular end-diastole volume (EDV), left ventricular ESV, and wall motion were evaluated using the Extended MR Workspace (Royal Philips).

Delayed contrast-enhanced imaging was performed 10–15 min after the first-pass perfusion using a two-dimensional segmented inversion recovery gradient-echo pulse sequence in continuous short-axis, four-chamber, and two-chamber long-axis views with full coverage of the LV to determine the infarct size. The FA was 15°, with TR 5.1 ms, TE 2.5 ms, FOV 255 mm×255 mm, and slice thickness 8 mm. The inversion time was chosen to minimize the signal from normal myocardium. A semiautomatic approach was used to quantify hyper-enhanced myocardium: epicardial and endocardial contours were drawn manually, and regions of interest were placed in hyper-enhanced and normal myocardium by the built-in software. Subsequently, areas of delayed enhancing myocardium were automatically segmented using a full-width at half-maximum algorithm. The threshold could be manually overridden if necessary to exclude significant artifacts. Infarct size was automatically calculated as the ratio of area of the myocardium with delayed enhancement to the area of LV myocardium in each slice from the short-axis delayed-enhancement images. Total infarct size was calculated by summation of all slice volumes with hyper-enhancement and divided by slice number. Infarct size change was defined as the difference in infarct size after cell transplantation compared with that at baseline.

Histology

Hearts were excised and cut into serial slices perpendicular to their longitudinal axis. Representative samples were selected from the infarct zone and scar tissue. All tissues were fixed for >24 h in 10% buffered formalin, embedded in paraffin, and processed for pathological analysis.

Formalin-fixed 4 μm thick sections were used for immunohistochemistry using various antibodies, with anti-mouse and anti-rabbit secondary antibodies (PV-6000; Zhongshan Golden Bridge Bio-technology, Beijing).

Arterioles in the infarct were identified as staining positive for α-smooth muscle actin (rabbit polyclonal anti-α-smooth muscle actin antibody, α-SMA, ab5694; Abcam, UK) and as having a visible lumen with a diameter between 10 and 100 μm (Christman et al., 2004; Kellar et al., 2001). Arteriole density was calculated as the average number of arterioles in the total infarct area, out of five representative slides per sample. Capillary density in the infarct was evaluated using rabbit polyclonal anti-von Willebrand factor antibody (vWf, ab6994; Abcam) and myocytes were identified using mouse monoclonal troponin T antibody (cTnT; ab10214; Abcam). Immunofluorescence co-staining was carried out using mouse monoclonal anti-human nuclear antigen antibody (ab220202; Abcam) and rabbit polyclonal anti-α-SMA antibody (ab5694; Abcam) to evaluate the retention and differentiation of hUMSCs in swine hearts. Microscopic evaluation and image acquisition were performed using an Olympus confocal microscope (FV1000-D IX81; Olympus, Japan), and Image-Pro Plus 6.0 software was used for quantification. Each section was counted in five randomly selected areas from the infarct zone under a light microscope and averaged among five sections for each sample. The primary antibody was omitted as a negative control.

Statistical analysis

The impacts of the cell therapies on phenotypic changes over time were analyzed by ANOVA with repeated measures. Multiple testing between groups was assessed by repeated measures ANOVA with Bonferroni correction. Actual *P* values are reported unadjusted. Preinjection versus post-injection parameters were compared using paired Student's *t*-test. Statistical analyses were carried out using the Statistics Package for Social Science software (version 22.0; IBM Corp., USA), and GraphPad Prism (version 7.0; GraphPad Software Inc., USA) and Adobe Illustrator (version CC 2018; Adobe Systems Incorporated, USA) were used to plot graphs. All values were expressed as mean±standard deviation, unless otherwise stated. A P value of <0.05 was considered statistically significant.

Compliance and ethics *The author(s) declare that they have no conflict of interest. All animal and human protocols were reviewed and approved by the Ethics Committee of Nanjing Drum Tower Hospital affiliated with Nanjing University Medical School, and conformed with the Helsinki Declaration of 1975 (as revised in 2008) concerning human and animal rights. We also followed our policy concerning informed consent, as can be seen at Springer.com.*

Acknowledgements *This work was supported by the Key Research Program of the Chinese Academy of Sciences (ZDRW-ZS-2016-2-2), the National Key Research and Development Program of China (2016YFC1000808), the National Natural Science Foundation of China (81370239), the Key Project supported by Medical Science and Technology Development Foundation, Nanjing Department of Health (201605016), the Key Project supported by Nanjing Medical Science and Technique Development Foundation (QRX17044),and the Youth Innovation Promotion Association CAS Project (2016096).*

References

Araña, M., Gavira, J.J., Peña, E., González, A., Abizanda, G., Cilla, M., Pérez, M.M., Albiasu, E., Aguado, N., Casado, M., et al. (2014). Epicardial delivery of collagen patches with adipose-derived stem cells in rat and minipig models of chronic myocardial infarction. Biomaterials 35, 143–151.

Araña, M., Peña, E., Abizanda, G., Cilla, M., Ochoa, I., Gavira, J.J., Espinosa, G., Doblaré, M., Pelacho, B., and Prosper, F. (2013). Preparation and characterization of collagen-based ADSC-carrier sheets for cardiovascular application. Acta Biomater 9, 6075–6083.

Behfar, A., Crespo-Diaz, R., Terzic, A., and Gersh, B.J. (2014). Cell therapy for cardiac repair—Lessons from clinical trials. Nat Rev Cardiol 11, 232–246.

Beltrami, A.P., Urbanek, K., Kajstura, J., Yan, S.M., Finato, N., Bussani, R., Nadal-Ginard, B., Silvestri, F., Leri, A., Beltrami, C.A., et al. (2001). Evidence that human cardiac myocytes divide after myocardial infarction. N Engl J Med 344, 1750–1757.

Blackburn, N.J.R., Sofrenovic, T., Kuraitis, D., Ahmadi, A., McNeill, B., Deng, C., Rayner, K.J., Zhong, Z., Ruel, M., and Suuronen, E.J. (2015). Timing underpins the benefits associated with injectable collagen biomaterial therapy for the treatment of myocardial infarction. Biomaterials 39, 182–192.

Bollini, S., Smits, A.M., Balbi, C., Lazzarini, E., and Ameri, P. (2018). Triggering endogenous cardiac repair and regeneration via extracellular vesicle-mediated communication. Front Physiol 9, 1497.

Buikema, J.W., Van Der Meer, P., Sluijter, J.P.G., and Domian, I.J. (2013). Concise review: Engineering myocardial tissue: The convergence of stem cells biology and tissue engineering technology. Stem Cells 31, 2587–2598.

Chachques, J.C., Trainini, J.C., Lago, N., Masoli, O.H., Barisani, J.L., Cortes-Morichetti, M., Schussler, O., and Carpentier, A. (2007). Myocardial assistance by grafting a new bioartificial upgraded myocardium (magnum clinical trial): One year follow-up. Cell Transplant 16, 927–934.

Chachques, J.C., Trainini, J.C., Lago, N., Cortes-Morichetti, M., Schussler, O., and Carpentier, A. (2008). Myocardial assistance by grafting a new bioartificial upgraded myocardium (magnum trial): Clinical feasibility study. Ann Thorac Surg 85, 901–908.

Chang, M.Y., Huang, T.T., Chen, C.H., Cheng, B., Hwang, S.M., and Hsieh, P.C.H. (2016). Injection of human cord blood cells with hyaluronan improves postinfarction cardiac repair in pigs. Stem Cells Transl Med 5, 56–66.

Chen, A.J., Pi, J.K., Hu, J.G., Huang, Y.Z., Gao, H.W., Li, S.F., Li-Ling, J., and Xie, H.Q. (2020). Identification and characterization of two morphologically distinct stem cell subpopulations from human urine samples. Sci China Life Sci 62, 712–723.

Chen, C.H., Chang, M.Y., Wang, S.S., and Hsieh, P.C.H. (2014). Injection of autologous bone marrow cells in hyaluronan hydrogel improves cardiac performance after infarction in pigs. Am J Physiol-Heart Circ Physiol 306, H1078–H1086.

Chiu, L.L.Y., Reis, L.A., Momen, A., and Radisic, M. (2012). Controlled release of thymosin β4 from injected collagen-chitosan hydrogels promotes angiogenesis and prevents tissue loss after myocardial infarction. Regen Med 7, 523–533.

Christman, K.L., Vardanian, A.J., Fang, Q., Sievers, R.E., Fok, H.H., and Lee, R.J. (2004). Injectable fibrin scaffold improves cell transplant survival, reduces infarct expansion, and induces neovasculature formation in ischemic myocardium. J Am Coll Cardiol 44, 654–660.

Dixit, P., and Katare, R. (2015). Challenges in identifying the best source of stem cells for cardiac regeneration therapy. Stem Cell Res Ther 6, 26.

Eschenhagen, T., Bolli, R., Braun, T., Field, L.J., Fleischmann, B.K., Frisén, J., Giacca, M., Hare, J.M., Houser, S., Lee, R.T., et al. (2017). Cardiomyocyte regeneration: A consensus statement. Circulation 136, 680–686.

Fukushima, S., Sawa, Y., and Suzuki, K. (2013). Choice of cell-delivery route for successful cell transplantation therapy for the heart. Future Cardiol 9, 215–227.

Gaballa, M.A., Sunkomat, J.N.E., Thai, H., Morkin, E., Ewy, G., and Goldman, S. (2006). Grafting an acellular 3-dimensional collagen scaffold onto a non-transmural infarcted myocardium induces neo-angiogenesis and reduces cardiac remodeling. J Heart Lung Transplant 25, 946–954.

Gao, J., Liu, J., Gao, Y., Wang, C., Zhao, Y., Chen, B., Xiao, Z., Miao, Q., and Dai, J. (2011). A myocardial patch made of collagen membranes loaded with collagen-binding human vascular endothelial growth factor accelerates healing of the injured rabbit heart. Tissue Eng Part A 17, 2739–2747.

Gautam, S., Chou, C.F., Dinda, A.K., Potdar, P.D., and Mishra, N.C. (2014). Surface modification of nanofibrous polycaprolactone/gelatin composite scaffold by collagen type I grafting for skin tissue engineering. Mater Sci Eng C 34, 402–409.

Gelse, K., Pöschl, E., and Aigner, T. (2003). Collagens—Structure, function, and biosynthesis. Adv Drug Deliv Rev 55, 1531–1546.

Golpanian, S., Wolf, A., Hatzistergos, K.E., and Hare, J.M. (2016). Rebuilding the damaged heart: Mesenchymal stem cells, cell-based therapy, and engineered heart tissue. Physiol Rev 96, 1127–1168.

Han, S., Xiao, Z., Li, X., Zhao, H., Wang, B., Qiu, Z., Li, Z., Mei, X., Xu, B., Fan, C., et al. (2018). Human placenta-derived mesenchymal stem cells loaded on linear ordered collagen scaffold improves functional recovery after completely transected spinal cord injury in canine. Sci China Life Sci 61, 2–13.

Holladay, C.A., Duffy, A.M., Chen, X., Sefton, M.V., O'Brien, T.D., and Pandit, A.S. (2012). Recovery of cardiac function mediated by MSC and interleukin-10 plasmid functionalised scaffold. Biomaterials 33, 1303–1314.

Hou, D., Youssef, E.A., Brinton, T.J., Zhang, P., Rogers, P., Price, E.T., Yeung, A.C., Johnstone, B.H., Yock, P.G. and March, K.L. (2005). Radiolabeled cell distribution after intramyocardial, intracoronary, and interstitial retrograde coronary venous delivery: Implications for current clinical trials. Circulation 112, I150–1156.

Jansen Of Lorkeers, S.J., Eding, J.E.C., Vesterinen, H.M., van der Spoel, T. I.G., Sena, E.S., Duckers, H.J., Doevendans, P.A., Macleod, M.R., and Chamuleau, S.A.J. (2015). Similar effect of autologous and allogeneic cell therapy for ischemic heart disease. Circ Res 116, 80–86.

Jeevanantham, V., Butler, M., Saad, A., Abdel-Latif, A., Zuba-Surma, E.K., and Dawn, B. (2012). Adult bone marrow cell therapy improves survival and induces long-term improvement in cardiac parameters. Circulation 126, 551–568.

Jiang, P., Tang, X., Wang, H., Dai, C., Su, J., Zhu, H., Song, M., Liu, J., Nan, Z., Ru, T., et al. (2019). Collagen-binding basic fibroblast growth factor improves functional remodeling of scarred endometrium in uterine infertile women: A pilot study. Sci China Life Sci 62, 1617–1629.

Keith, M.C.L., Tang, X.L., Tokita, Y., Li, Q., Ghafghazi, S., Moore Joseph, I., Hong, K.U., Elmore, B., Amraotkar, A., Ganzel, B.L., et al. (2015). Safety of intracoronary infusion of 20 million C-kit positive human cardiac stem cells in pigs. PLoS ONE 10, e0124227.

Kellar, R.S., Landeen, L.K., Shepherd, B.R., Naughton, G.K., Ratcliffe, A., and Williams, S.K. (2001). Scaffold-based three-dimensional human fibroblast culture provides a structural matrix that supports angiogenesis in infarcted heart tissue. Circulation 104, 2063–2068.

Kijeńska, E., Prabhakaran, M.P., Swieszkowski, W., Kurzydlowski, K.J., and Ramakrishna, S. (2012). Electrospun bio-composite P(LLA-CL)/collagen I/collagen III scaffolds for nerve tissue engineering. J Biomed Mater Res 100B, 1093–1102.

Lin, H. (2019). Transplantation of adult spinal cord tissue: Transection spinal cord repair and potential clinical translation. Sci China Life Sci 62, 870–872.

Lin, Y.D., Yeh, M.L., Yang, Y.J., Tsai, D.C., Chu, T.Y., Shih, Y.Y., Chang, M.Y., Liu, Y.W., Tang, A.C.L., Chen, T.Y., et al. (2010). Intramyocardial peptide nanofiber injection improves postinfarction ventricular remodeling and efficacy of bone marrow cell therapy in pigs. Circulation 122, S132–S141.

Liu, B., Duan, C.Y., Luo, C.F., Ou, C.W., Wu, Z.Y., Zhang, J.W., Ni, X.B., Chen, P.Y., and Chen, M.S. (2016). Impact of timing following acute myocardial infarction on efficacy and safety of bone marrow stem cells therapy: A network meta-analysis. Stem Cells Int 2016, 1–11.

Mahmoudi, M., Yu, M., Serpooshan, V., Wu, J.C., Langer, R., Lee, R.T., Karp, J.M., and Farokhzad, O.C. (2017). Multiscale technologies for treatment of ischemic cardiomyopathy. Nat Nanotech 12, 845–855.

Marquardt, L.M., and Heilshorn, S.C. (2016). Design of injectable materials to improve stem cell transplantation. Curr Stem Cell Rep 2, 207–220.

Martin-Rendon, E., Brunskill, S.J., Hyde, C.J., Stanworth, S.J., Mathur, A., and Watt, S.M. (2008). Autologous bone marrow stem cells to treat acute myocardial infarction: A systematic review. Eur Heart J 29, 1807–1818.

Maureira, P., Marie, P.Y., Yu, F., Poussier, S., Liu, Y., Groubatch, F., Falanga, A., and Tran, N. (2012). Repairing chronic myocardial infarction with autologous mesenchymal stem cells engineered tissue in rat promotes angiogenesis and limits ventricular remodeling. J Biomed Sci 19, 93.

Mokashi, S.A., Guan, J., Wang, D., Tchantchaleishvili, V., Brigham, M., Lipsitz, S., Lee, L.S., Schmitto, J.D., Bolman Iii, R.M., Khademhosseini, A., et al. (2010). Preventing cardiac remodeling: The combination of cell-based therapy and cardiac support therapy preserves left ventricular function in rodent model of myocardial ischemia. J Thorac Cardiovasc Surg 140, 1374–1380.

Nguyen, P.K., Neofytou, E., Rhee, J.W., and Wu, J.C. (2016). Potential strategies to address the major clinical barriers facing stem cell regenerative therapy for cardiovascular disease. JAMA Cardiol 1, 953–962.

Paiva, L., Providência, R., Barra, S., Dinis, P., Faustino, A.C., and Gonçalves, L. (2015). Universal definition of myocardial infarction: Clinical insights. Cardiology 131, 13–21.

Perea-Gil, I., Prat-Vidal, C., and Bayes-Genis, A. (2015). *In vivo* experience with natural scaffolds for myocardial infarction: The times they are a-changin. Stem Cell Res Ther 6, 248.

Radhakrishnan, J., Krishnan, U.M., and Sethuraman, S. (2014). Hydrogel based injectable scaffolds for cardiac tissue regeneration. Biotech Adv 32, 449–461.

Sanganalmath, S.K., and Bolli, R. (2013). Cell therapy for heart failure. Circ Res 113, 810–834.

Sepantafar, M., Maheronnaghsh, R., Mohammadi, H., Rajabi-Zeleti, S., Annabi, N., Aghdami, N., and Baharvand, H. (2016). Stem cells and injectable hydrogels: Synergistic therapeutics in myocardial repair. Biotech Adv 34, 362–379.

Serpooshan, V., Zhao, M., Metzler, S.A., Wei, K., Shah, P.B., Wang, A., Mahmoudi, M., Malkovskiy, A.V., Rajadas, J., Butte, M.J., et al. (2013). The effect of bioengineered acellular collagen patch on cardiac remodeling and ventricular function post myocardial infarction. Biomaterials 34, 9048–9055.

Shafy, A., Fink, T., Zachar, V., Lila, N., Carpentier, A., and Chachques, J.C. (2013). Development of cardiac support bioprostheses for ventricular restoration and myocardial regeneration. Eur J Cardiothorac Surg 43, 1211–1219.

Shen, H., Chen, X., Li, X., Jia, K., Xiao, Z., and Dai, J. (2019). Transplantation of adult spinal cord grafts into spinal cord transected rats improves their locomotor function. Sci China Life Sci 62, 725–733.

Shi, C., Li, Q., Zhao, Y., Chen, W., Chen, B., Xiao, Z., Lin, H., Nie, L., Wang, D., and Dai, J. (2011). Stem-cell-capturing collagen scaffold promotes cardiac tissue regeneration. Biomaterials 32, 2508–2515.

Shiba, Y., Gomibuchi, T., Seto, T., Wada, Y., Ichimura, H., Tanaka, Y., Ogasawara, T., Okada, K., Shiba, N., Sakamoto, K., et al. (2016). Allogeneic transplantation of iPS cell-derived cardiomyocytes regenerates primate hearts. Nature 538, 388–391.

Thygesen, K., Alpert, J.S., Jaffe, A.S., Simoons, M.L., Chaitman, B.R., White, H.D., Thygesen, K., Alpert, J.S., White, H.D., Jaffe, A.S., et al. (2012). Third universal definition of myocardial infarction. J Am Coll Cardiol 60, 1581–1598.

Wall, S.T., Yeh, C.C., Tu, R.Y.K., Mann, M.J., and Healy, K.E. (2010). Biomimetic matrices for myocardial stabilization and stem cell transplantation. J Biomed Mater Res 95A, 1055–1066.

Wang, B., Han, J., Gao, Y., Xiao, Z., Chen, B., Wang, X., Zhao, W., and Dai, J. (2007). The differentiation of rat adipose-derived stem cells into OEC-like cells on collagen scaffolds by co-culturing with OECs. Neurosci Lett 421, 191–196.

Wu, W.Q., Peng, S., Song, Z.Y., and Lin, S. (2019). Collagen biomaterial for the treatment of myocardial infarction: An update on cardiac tissue engineering and myocardial regeneration. Drug Deliv Transl Res 9, 920–934.

Xiang, Z., Liao, R., Kelly, M.S., and Spector, M. (2006). Collagen-GAG scaffolds grafted onto myocardial infarcts in a rat model: A delivery vehicle for mesenchymal stem cells. Tissue Eng 12, 2467–2478.

Xu, J., Xiong, Y.Y., Li, Q., Hu, M.J., Huang, P.S., Xu, J.Y., Tian, X.Q., Jin, C., Liu, J.D., Qian, L., et al. (2019). Optimization of timing and times for administration of atorvastatin-pretreated mesenchymal stem cells in a preclinical model of acute myocardial infarction. Stem Cells Transl Med 8, 1068–1083.

Xu, Y., Dong, S., Zhou, Q., Mo, X., Song, L., Hou, T., Wu, J., Li, S., Li, Y., Li, P., et al. (2014). The effect of mechanical stimulation on the maturation of tdscs-poly(l-lactide-co-e-caprolactone)/collagen scaffold constructs for tendon tissue engineering. Biomaterials 35, 2760–2772.

Zhao, Y., Tang, F., Xiao, Z., Han, G., Wang, N., Yin, N., Chen, B., Jiang, X., Yun, C., Han, W., et al. (2017). Clinical study of neuroregen scaffold combined with human mesenchymal stem cells for the repair of chronic complete spinal cord injury. Cell Transplant 26, 891–900.